Available online at www.sciencedirect.com
ScienceDirect
Journal of the European Ceramic Society 27 (2007) 2325–2331
www.elsevier.com/locate/jeurceramsoc

Diopside–Ca-Tschermak clinopyroxene based glass–ceramics processed via sintering and crystallization of glass powder compacts

A. Goel [a], D.U. Tulyaganov [b], S. Agathopoulos [c], M.J. Ribeiro [d], R.N. Basu [e], J.M.F. Ferreira [a,*]

[a] *Department of Ceramics and Glass Engineering, University of Aveiro, CICECO, 3810-193 Aveiro, Portugal*
[b] *Scientific Research Institute of Space Engineering, 700128 Tashkent, Uzbekistan*
[c] *Department of Materials Science and Engineering, University of Ioannina, Greece, GR-451 10 Ioannina, Greece*
[d] *UIDM, ESTG, Polytechnic Institute of Viana do Castelo, 4900 Viana do Castelo, Portugal*
[e] *FCBS, Central Glass and Ceramic Research Institute, Kolkata 700032, India*

Received 8 April 2006; received in revised form 17 July 2006; accepted 21 July 2006
Available online 11 September 2006

Abstract

The suitability of three new glass compositions for producing diopside–Ca-Tschermak clinopyroxene based glass–ceramics (GCs) was investigated. With respect to the formula of diopside, the first investigated composition resulted from the substitution $0.2(Si^{4+} + Mg^{2+}) \leftrightarrow 0.4\,Al^{3+}$, which leads to a composition of 80 mol.% diopside and 20 mol.% Ca-Tschermak. The substitutions in the second compositions were $0.25(Ca^{2+} + Si^{4+}) \leftrightarrow 0.25(Y^{3+} + B^{3+})$ and $0.2(Si^{4+} + Mg^{2+}) \leftrightarrow 0.4Al^{3+}$, and in the third composition $0.2Ba^{2+} \leftrightarrow 0.2Ca^{2+}$ and $0.2(Si^{4+} + Mg^{2+}) \leftrightarrow 0.2(B^{3+} + Al^{3+})$. The influence of these substitutions on glass crystallization and the properties of the GCs produced between 850 and 1000 °C was experimentally investigated. The experimental results showed that the easily cast glasses, after melting at 1580 °C for 1 h, are prone to surface crystallization. Augite is predominantly crystallized, but Ca- and Ba-aluminosilicates can also form, according to the substitutions. The stability of the assemblage of the crystalline phases over a wide temperature range (850–1000 °C) and prolonged heat treatment (up to 50 h) and the properties of the produced GCs indicate a high potential of these compositions for several functional applications.

Keywords: Sintering; Mechanical properties; Glass–ceramics; Diopside–Ca-Tschermak; Functional applications

1. Introduction

Pyroxenes are major constituents of the earth's crust and of the upper mantle to depths of 400 km.[1] They occur in a wide variety of geological settings, both igneous and metamorphic. Pyroxenes have the general formula of $M_1M_2(Si,Al)_2O_6$, where M_1 is usually Ca^{2+}, Na^{+}, Fe^{2+} and Mg^{2+}, and more rarely Zn^{2+}, Mn^{2+} and Li^{+}, and M_2 refers to smaller ions, such as Cr^{3+}, Al^{3+}, Fe^{3+}, Mg^{2+}, Mn^{2+}, Sc^{3+}, Ti^{4+}, V^{5+} and even Fe^{2+}. The chain silicate structure of pyroxenes enables incorporation of various cations in their structure resulting in minerals found in abundance in the nature, such as diopside ($CaMgSi_2O_6$), hedenbergite ($CaFeSi_2O_6$), aegirine ($NaFeSi_2O_6$), jadeite ($NaAlSi_2O_6$), spodumene ($LiAlSi_2O_6$), augite $(Ca,Na)(Mg,Fe,Al,Ti)(Si,Al)_2O_6$, etc. Several papers have described the structural features of this family of compounds,[2–5] whose detailed description is, however, beyond the scope of the present paper.

The Ca-aluminium bearing monoclinic clinopyroxene, known as Ca-Tschermak ($CaAl_2SiO_6$), is representative of the pyroxene group where both Si and Al are in tetrahedral sites. Diopside forms solid solution with Ca-Tschermak with a general formula of $Ca[Mg_{1-x}Al_x](Si_{1-x/2}Al_{x/2})_2O_6$, where the square brackets and the parentheses denote the octahedral and the tetrahedral sublattices, respectively.[1] Cation substitution is governed by Tschermak's substitution, concisely represented by the scheme $(Si^{4+}) + [Mg^{2+}] \leftrightarrow (Al^{3+}) + [Al^{3+}]$.

The amount of $CaAl_2SiO_6$ in a pyroxene glass–ceramic structure depends on the composition of the parent glass and the crystallization parameters. Kushiro[6] and Schairer and Yoder[7] have demonstrated that the maximum concentration of $CaAl_2SiO_6$, which can be accommodated in diopside, is 20%. Salama et

* Corresponding author. Tel.: +351 234 370242; fax: +351 234 425300.
E-mail address: jmf@cv.ua.pt (J.M.F. Ferreira).

0955-2219/$ – see front matter © 2006 Elsevier Ltd. All rights reserved.
doi:10.1016/j.jeurceramsoc.2006.07.016

al.[8] have investigated the crystallization of glasses based on the ternary system of diopside–Ca-Tschermak–fluorapatite. They demonstrated that the limit of isomorphic substitution of Ca-Tschermak's component in diopside structure is 25%. Above that limit, gehlenite ($Ca_2Al_2SiO_7$) forms. The coefficient of thermal expansion (CTE) and the microhardness of the produced glass–ceramics (GCs) increased with increasing the ratio of Ca-Tschermak/diopside.

It is known that the properties of GCs based on clinopyroxenes and particularly the diopside–Ca-Tschermak solid solutions can be highly controlled due to their particular structural features.[8–12] The wide stability range of clinopyroxenes, the broad spectrum of their chemistry, the possibility of achieving desired physical properties and the high chemical durability have been considered for producing GCs for a large variety of applications.[10–15] Accordingly, it is believed that novel alternatives of synthetic clinopyroxenes produced via GC-route can yield interesting materials for several functional applications.

In this study, three novel glass compositions based on diopside were investigated, denoted for simplicity purposes as DT-1, DT-2 and DT-3. Table 1 presents their chemical composition. The composition DT-1 comprised 80 mol.% diopside and 20 mol.% Ca-Tschermak. With regard to the design of this composition, it actually derives from diopside if we substitute $0.2(Si^{4+} + Mg^{2+})$ with $0.4Al^{3+}$. More complex substitutions were attempted in the composition DT-2, where $0.25(Ca^{2+} + Si^{4+})$ was substituted by $0.25(Y^{3+} + B^{3+})$ and $0.2(Si^{4+} + Mg^{2+})$ by $0.4Al^{3+}$. In the composition DT-3, $0.2Ba^{2+}$ substituted $0.2Ca^{2+}$ and $0.2(Si^{4+} + Mg^{2+})$ was substituted by $0.2(B^{3+} + Al^{3+})$. The incorporation of B_2O_3 in the compositions DT-2 and DT-3 had a dual aim: to satisfy the overall charge balance in the system, and under the perspective of technology, to decrease the viscosity of glass melts and to facilitate diffusion. The experimental results aim to present the influence of the above substitutions on the crystallization and the properties of the resultant GCs. To enhance the potential applications of the produced GCs, and particularly towards the possibility of using the produced materials as SOFC-sealants or for the immobilization of radionuclides,[16–18] we incorporated in the batches a small amount of NiO (1 wt.%), considering that NiO will favour the adhesion of the resultant GCs to metals. For simplicity purposes, the designations DT-1, DT-2, and DT-3 correspond to both the glasses and the respective GCs.

2. Materials and experimental procedure

Powders of technical grade SiO_2 (purity >99.5%) and $CaCO_3$ (>99.5%), and of reactive grade H_3BO_3, Al_2O_3, MgO, Y_2O_3, $BaCO_3$, and NiO were used. Homogeneous mixtures of batches (~100 g), obtained by ball milling, were preheated at 900 °C for 1 h for decarbonization and then melted in alumina crucibles at 1580 °C for 1 h, in air.

Glasses in bulk form were produced by casting the molten glass on preheated (500 °C) bronze moulds and subsequent immediate annealing at 550 °C (i.e. close to the transformation temperature T_g) for 1 h. Glasses in frit form were also obtained by quenching of the melts in cold water. The frit was dried and then milled in a high-speed porcelain mill. For the thermal analysis, different fractions of particles retained on different sieves −1000 + 500 μm, −500 + 315 μm, and −315 + 90 μm were collected. For the production of the samples, only the finest powders were used. Those fine powders were granulated (by stirring in a mortar) in a 5 vol.% polyvinyl alcohol solution (PVA, Merck; the solution of PVA was made by dissolution in warm water) in a proportion of 97.5 wt.% of frit and 2.5 wt.% of PVA. Rectangular bars with dimensions of 4 mm × 5 mm × 50 mm were prepared by uniaxial pressing (80 MPa). The bars were sintered at four different temperatures (i.e. 850, 900, 950, and 1000 °C) in air in an electrical laboratory furnace. The soaking time at the sintering temperature was 1 h. A slow heating and cooling rate of 2 K/min was used to prevent deformation of the samples.

In this study, the following techniques and apparatuses were employed. The light scattering technique was employed to determine the particle size distribution of the fine powders (Coulter LS 230, UK, Fraunhofer optical model). Differential thermal analysis (DTA) was carried out in air (Netzsch 402 EP, Germany) with a heating rate of 5 K/min. Dilatometry measurements were done with prismatic samples with cross-section of 4 mm × 5 mm (Bahr Thermo Analyse DIL 801 L, Germany, heating rate of 5 K/min). The crystalline phases were identi-

Table 1
Compositions of the parent glasses

Glass	MgO	CaO	BaO	SiO_2	B_2O_3	Al_2O_3	Y_2O_3
DT-1, $CaMg_{0.8}Al_{0.4}Si_{1.8}O_6$							
wt.%	14.87	25.86	–	49.87	–	9.40	–
mol.%	21.05	26.32	–	47.37	–	5.26	–
mol ratio	4	5	–	9	–	1	–
DT-2, $Ca_{0.75}Y_{0.25}Mg_{0.8}Al_{0.4}Si_{1.55}B_{0.25}O_6$							
wt.%	14.35	18.70	–	41.44	3.87	9.07	12.55
mol.%	22.53	21.13	–	43.66	3.52	5.63	3.52
mol ratio	6.4	6	–	12.4	1	1.60	1
DT-3, $Ca_{0.8}Ba_{0.2}Mg_{0.8}Al_{0.2}B_{0.2}Si_{1.8}O_6$							
wt.%	13.83	19.24	13.15	46.40	2.98	4.37	–
mol.%	21.05	21.05	5.26	47.37	2.63	2.63	–
mol ratio	8	8	2	18	1	1	–

Note: 1.00 wt.% NiO was added to the batches.

fied by X-ray diffraction analysis (XRD, Rigaku Geigerflex D/Mac, C Series, Cu Kα radiation, Japan). Copper Kα radiation ($\lambda = 1.5406$ nm) produced at 30 kV and 25 mA scanned the range of diffraction angles (2θ) between 10° and 60° with a 2θ-step of 0.02° s^{-1}. The phases were identified by comparing the experimental diffractograms to patterns of standards complied by the International Centre for Diffraction Data (ICDD). Microstructure observations were done at polished (mirror finishing) and then etched (by immersion in 2 vol.% HF solution for 20 s) surfaces of samples by field emission scanning electron microscopy (FE–SEM Hitachi S-4100, Japan; 25 kV acceleration voltage, beam current 10 μA) under secondary electron mode. Energy dispersive spectroscopy (EDS) was employed for chemical analysis. Archimedes method (i.e. immersion in diethyl phthalate) was employed to measure the apparent density of the samples. The mechanical properties were evaluated by measurements of three-point bending strength of rectified parallelepiped bars (3 mm × 4 mm × 50 mm) of sintered GCs (Shimadzu Autograph AG 25 TA; 0.5 mm/min displacement). The linear shrinkage during sintering was calculated from the difference of the dimensions between the green and the sintered bars. The mean values and the standard deviations presented for density, bending strength and linear shrinkage have been obtained from (at least) 10 different samples.

3. Results and discussion

3.1. Characterization of glasses—thermal analysis

All the three investigated compositions were suitable for easy cast after 1 h of melting at 1580 °C, resulting in homogenous transparent, bubble-free glasses with a dark colour of honey (likely due to the presence of NiO) and with no crystalline inclusions, as confirmed by X-ray and SEM analyses afterwards.

The curves of thermal expansion of the three cast-annealed bulk glasses are plotted in Fig. 1. The glass transition points (T_g) of the glasses DT-1, DT-2 and DT-3, determined from these curves, are 640, 630 and 600 °C, and their softening points (T_s) are 680, 660 and 650 °C, respectively. From the slope of the linear part of these curves (i.e. between 200 and 500 °C), the CTE values of the three glasses were calculated as 7.22×10^{-6}, 7.20×10^{-6}, and 7.51×10^{-6} °C^{-1}, respectively.

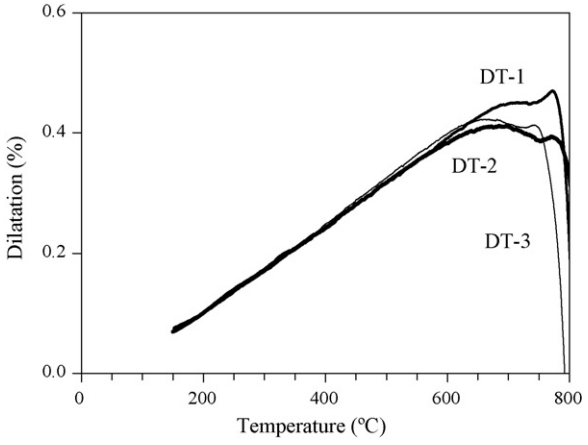

Fig. 1. Dilatometry curves of the as-cast and annealed bulk glasses.

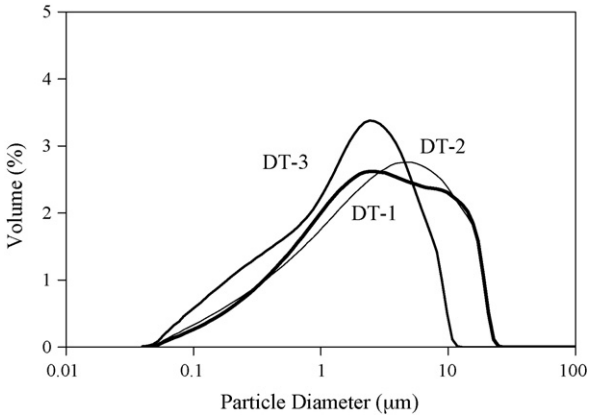

Fig. 2. Particle size distributions of milled glass fine powders used to prepare the glass-powder compacts.

The particle size distributions of the fine powders used to produce the samples of the glass-powder compacts are plotted in Fig. 2. The measured mean particle sizes were 4.73 μm for DT-1, 4.85 μm for DT-2, and 2.43 μm for DT-3. Fig. 3 presents the results of the differential thermal analysis of these fine powders. The strong exothermic reaction peaked at 920–925 °C is attributed to crystallization (T_p). Evidently, the intensity of the crystallization peaks diminishes from the glass DT-1 to the glass DT-3. In the plots of the DT-1 and DT-2 glasses, weak exothermic peaks at 860–875 °C precede the main crystallization peaks.

The influence of particle size on the DTA-curves was investigated by using coarse fractions of powder glass frits retained in the following pair sieves: −1000 + 500 μm, −500 + 315 μm, and −315 + 90 μm (Fig. 4). The plots in Fig. 4 in conjunction with the plots in Fig. 3 indicate that the coarser particles resulted

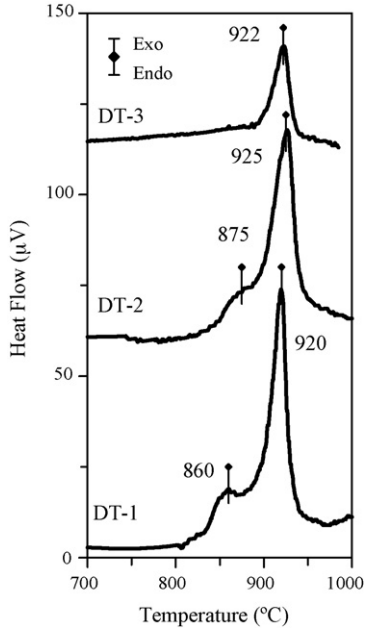

Fig. 3. Differential thermal analysis (DTA) of fine powders (see Fig. 2) of the investigated glasses.

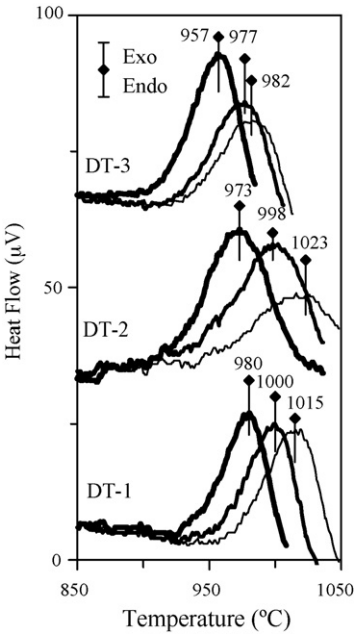

Fig. 4. Influence of particle size on the DTA of the investigated glasses (thick line: −315 + 90 μm; medium line: −500 + 315 μm; thin line: −1000 + 500 μm).

in a systematic and considerable shift of the principal crystallization peak to higher temperatures, while the intensity of the peaks generally tends to decrease. Thus, the preceding smaller crystallization peaks in Fig. 3 have been almost totally eliminated in the DTA-plots of the coarser particles (Fig. 4). The strong dependence of these thermographs on particle size suggests surface crystallization as the dominant crystallization mechanism of the investigated compositions.[9,19–21]

The results of dilatometry (i.e. the temperatures of T_g and T_s, Fig. 1) and DTA (i.e. the temperatures of T_p, Fig. 3) indicate that there is a relatively wide temperature gap between glass-transition point and crystallization temperature. These features suggest that densification should precede crystallization, justifying our decision to attempt the production of GCs via sintering and crystallization of glass-powder compacts from the fine glass powders (Fig. 2). This was proved afterwards by the sintering experiments presented in the following section. Accordingly, the temperatures of heat treatment of glass powder compacts to test the production and the properties of GCs were chosen to be between 850 and 1000 °C.[22]

3.2. Properties of sintered glass-powder compacts

The influence of temperature on the density, the shrinkage and the bending strength of glass-powder compacts is presented in the plots in Fig. 5. It is generally known that sintering starts at temperatures slightly higher than T_g and occurs due to viscous flow, which instigates coalescence of powder and removes the pores from the bulk of materials. The use of special additives, such as B_2O_3, and fine glass powders generally enhances sinterability.[15,19,22–24] The B_2O_3-containing compositions of DT-2 and DT-3 exhibited their highest values of density, shrinkage and bending strength in the temperature interval of

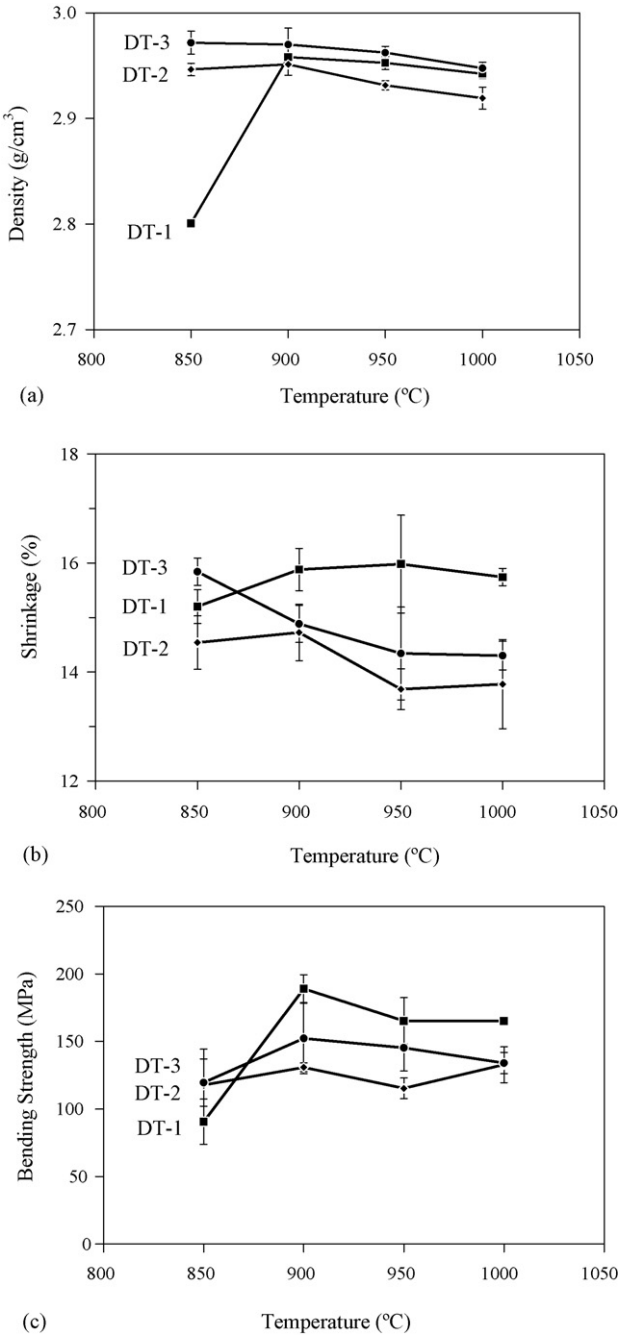

Fig. 5. Influence of the temperature on (a) density, (b) linear shrinkage, and (c) bending strength.

850–900 °C, evidencing highly sintered samples. The highest values of composition DT-1 were achieved in the interval of 900–950 °C, specifically density of 2.95–2.96 g/cm^3, shrinkage of 15.88–15.98%, and bending strength of 165–189 MPa. Further increase in temperature to 950 or 1000 °C did not considerably deteriorate the properties of the investigated compositions, since density and mechanical strength were generally maintained at the same level.

With regards to the thermal expansion of the produced GCs and particularly those sintered at 950 °C for 1 h, the CTE values determined by dilatometry measurements between 200 and

700 °C were 9.57×10^{-6} °C^{-1} for DT-1, 8.01×10^{-6} °C^{-1} for DT-2, and 9.62×10^{-6} °C^{-1} for DT-3.

3.3. Phase evolution under isothermal and non-isothermal heat treatment

The microstructure of the glass-powder compact samples sintered at 850 °C was discerned by SEM but the glassy phase dominated. The crystals were well developed at 900 °C (Fig. 6a) and even better at 950 °C (Fig. 6b–d). The images in Fig. 6 indicate, however, noticeable differences among the three investigated GCs. The results of X-ray diffraction analysis, presented in the diffractograms in Figs. 7 and 8 shed light in these differences and the evolution of phases.

The bars of DT-1 composition sintered at 850 °C for 1 h were completely amorphous. After heat treatment at 900 °C for 1 h, intensive and sharp peaks of augite were registered in the X-ray diffractograms, evidencing formation of diopside–Ca-Tschermak solid solution. Augite was also exclusively registered in the diffractograms of DT-1 samples heat treated at higher temperatures (950 and 1000 °C) or for longer times (up to 50 h) at 900 °C (Fig. 7a), where, the intensity of the XRD peaks was progressively increased. These results suggest that the composition DT-1 results in stable monomineral GCs of pyroxene augite. The results of X-ray agree fairly well with the SEM observations, since a well crystallized and almost monomineral GC is also suggested by the images in Fig. 6a and b.

The formation of single phase of augite [$Ca(Mg_{0.70}Al_{0.30})(Si_{1.70}Al_{0.30})O_6$] indicates that Al^{3+} occupied both octahedral (AlO_6) and tetrahedral (AlO_4) positions in the structure of that aluminous pyroxene. The small deviation from the theoretically designed diopside–Ca-Tschermak solid solution of $CaMg_{0.8}Al_{0.4}Si_{1.8}O_6$ (Table 1) can be due to uptake of Al_2O_3 from the alumina crucibles, which, according to EDS analysis, was determined as 1.5–2.0 wt.% Al_2O_3. The ability of aluminium to exist in the form of an intermediate oxide at both octahedral (AlO_6) and tetrahedral (AlO_4) positions in glass structures is known.[9–11,25] The formation of AlO_4 groups generally results in increase of glass viscosity and decrease of crystal growth rate.[8] Hence, higher T_g and T_s values along with more sluggish crystallization is expected for DT-1 glass than the DT-2 and DT-3 glasses.

Evidences of devitrification were observed after heat treatment at 850 °C for 1 h for both DT-2 and DT-3 samples. This result can explain the lower density and mechanical strength of the DT-1 bars sintered at 850 °C than the DT-2 and DT-3 ones (Fig. 5). Except for slight changes of peak intensities of the diffractograms, composition DT-2 exhibited remarkable stability of phase assemblage at different temperatures as well as under prolonged heat treatment at 900 °C for up to 50 h. Augite, anorthite, and yttrium oxide silicate were identified in the GCs of DT-2. Schairer and Yoder[7] have demonstrated that if the amount of $CaAl_2SiO_6$ (Ca-Tschermak) exceeds the solubility limit in the $CaMgSi_2O_6$–$CaAl_2SiO_6$ system, then Ca-aluminosilicate anorthite ($CaAl_2Si_2O_8$) might be formed.

The assemblage of phases in the GCs of DT-3 comprises augite, hexacelsian and celsian. The presence of the later two phases (which had strong peaks in the diffractograms) is due to the fact that crystallization of barium aluminosilicate glasses occurs faster than in the corresponding calcium or magnesium aluminosilicate glasses.[16,25,26] However, the ratio of the intensity of the peaks of augite over the peaks of Ba-aluminosilicates phases increases over prolonged heat treatment, suggesting for-

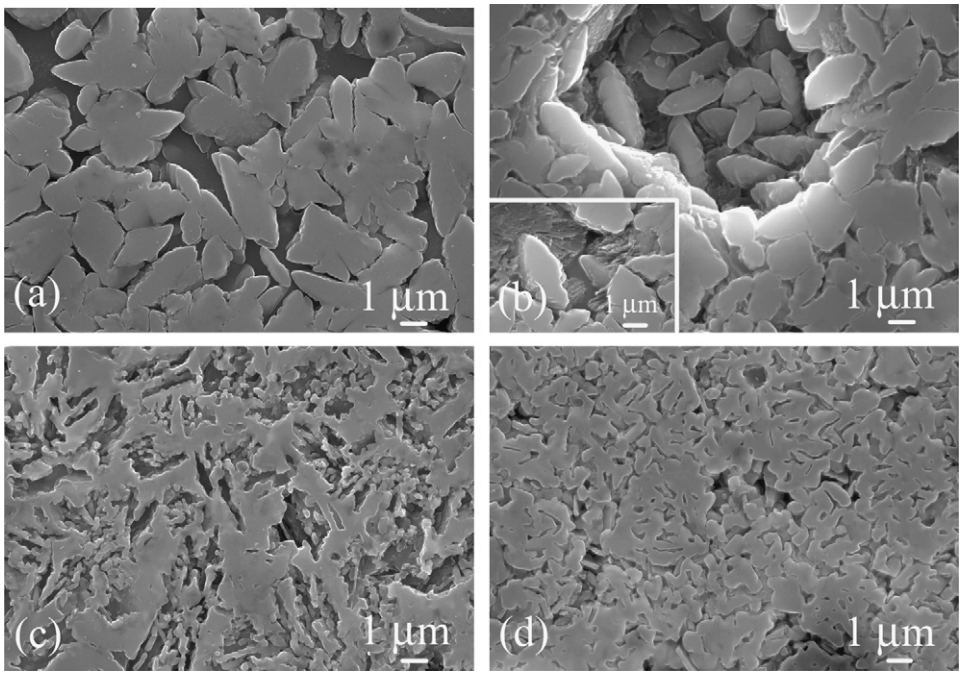

Fig. 6. Microstructure of glass–ceramics heat treated at different temperatures for 1 h after etching with 2 vol.% HF: (a) DT-1, 900 °C; (b) DT-1, 950 °C; (c) DT-2, 950 °C; (d) DT-3, 950 °C.

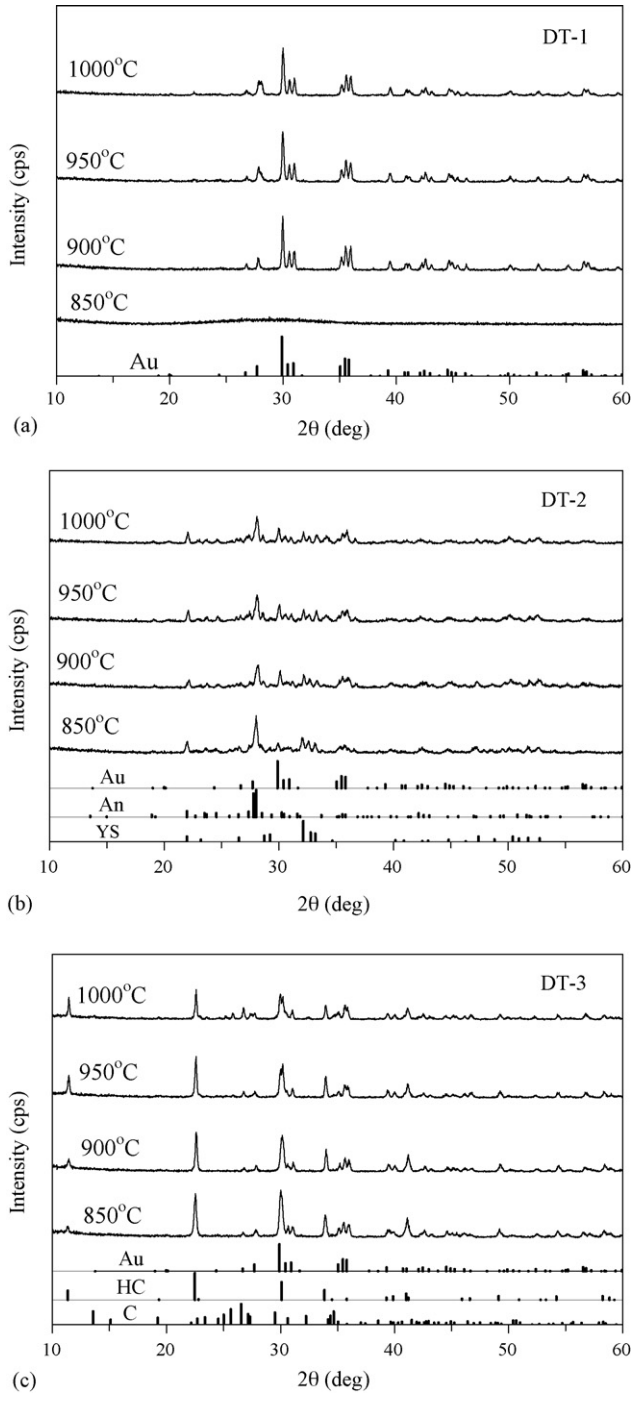

Fig. 7. X-ray diffracrograms of glass-powder compacts after heat treatment at different temperatures for 1 h. (a) DT-1, (b) DT-2, and (c) DT-3. (Au: augite ICDD card 01-078-1392; An: anorthite 00-041-1486; YS: yttrium oxide silicate ($Y_{4.67}(SiO_4)_3O$) 00-030-1457; HS: hexacelsian ($BaAl_2Si_2O_8$) 01-077-185; C: celsian ($BaAl_2Si_2O_8$) 00-038-1450. The spectra have not been normalized. Full scale 9000 cps.)

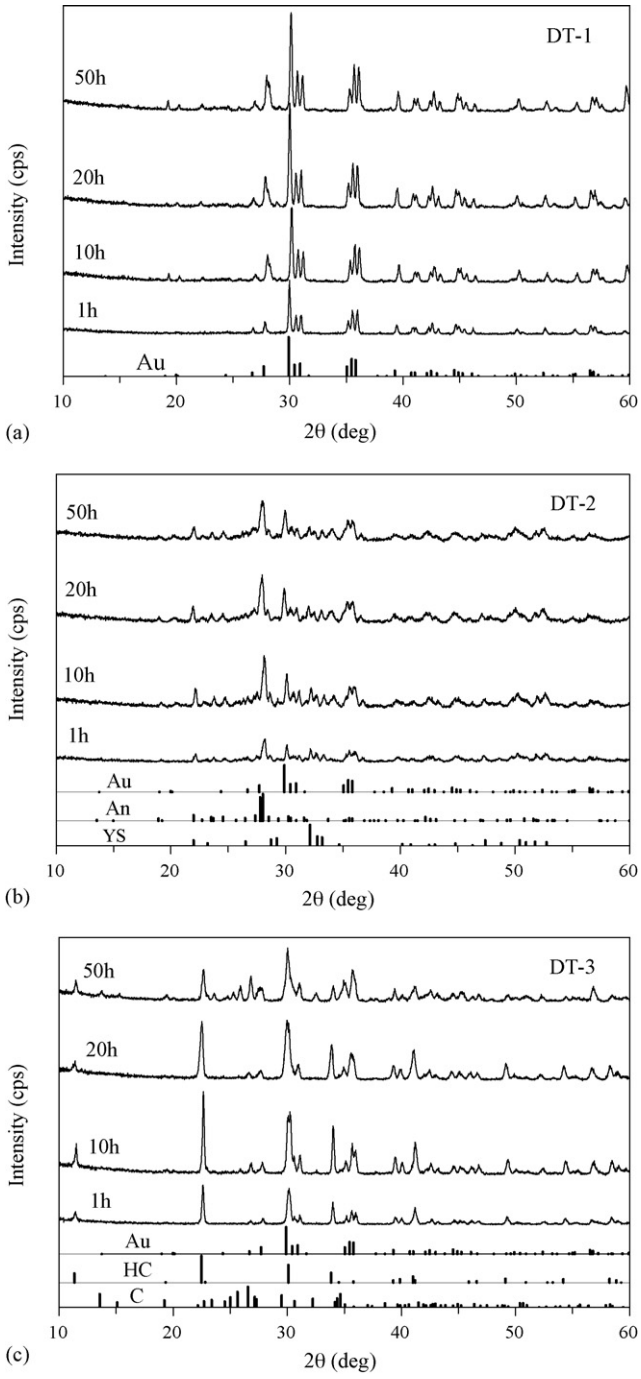

Fig. 8. X-ray diffractograms of glass-powder compacts after heat treatment at 900 °C for 1, 10, 20 and 50 h. (a) DT-1, (b) DT-2, and (c) DT-3. (Phase identification and scale are similar to those reported in the legend of Fig. 7.)

mation of augite at the expenses of these phases. Thus, the microstructure in Fig. 6d should be rather assigned to Ba-aluminosilicate associated phases than to augite. Accordingly, a mixed microstructure of augite and anorthite can be suggested for the microstructure of the GCs of DT-2 presented in Fig. 6c.

4. Conclusions

Three new glass compositions (DT-1, DT-2, DT-3) were investigated with regards to their suitability of producing diopside–Ca-Tschermak clinopyroxene based glass–ceramics. With respect to diopside, the substitutions attempted were $0.2(Si^{4+} + Mg^{2+}) \leftrightarrow 0.4Al^{3+}$ for DT-1, $0.25(Ca^{2+} + Si^{4+}) \leftrightarrow 0.25(Y^{3+} + B^{3+})$ and $0.2(Si^{4+} + Mg^{2+}) \leftrightarrow 0.4Al^{3+}$ for DT-2, and

$0.2Ba^{2+} \leftrightarrow 0.2Ca^{2+}$ and $0.2(Si^{4+} + Mg^{2+}) \leftrightarrow 0.2(B^{3+} + Al^{3+})$ for DT-3.

Glasses were suitable for easy cast after melting at 1580 °C for 1 h. Sintering and crystallization of glass-powder compacts is an appropriate processing route for producing glass–ceramics of these compositions because the experimental results showed that sintering precedes crystallization which occurs via surface crystallization mechanism.

With regards to the comparison of the three compositions, and particularly their potential application as SOFC-sealant materials (which was the main motivation for developing these new compositions), it is suggested that the monomineral composition, the phase stability over increasing of temperature and prolonged isothermal heat treatment, and the good matching of the CTE with the CTE of cubic zirconia (8YSZ) indicate a superiority of DT-1 than DT-2 and DT-3.

Acknowledgement

A. Goel is indebted for the research fellowship grant from CICECO.

References

1. Flemming, R. L. and Luth, R. W., ^{29}Si MAS NMR study of dioside–Ca-Tschermak clinopyroxenes: detecting both tetrahedral and octahedral Al substitution. *Am. Mineral.*, 2002, **87**, 25–36.
2. Tribaudino, M., A transmission electron microscope investigation of the $C2/c \rightarrow P2_1/c$ phase transition in clinopyroxenes along the diopside-enstatite ($CaMgSi_2O_6$–$Mg_2Si_2O_6$) join. *Am. Mineral.*, 2000, **85**, 707–715.
3. Cameron, M. and Papike, J. J., Structural and chemical variations in pyroxenes. *Am. Mineral.*, 1981, **66**, 1–50.
4. Barth, T. F., *Theoretical Petrology* (*2nd ed.*). Wiley, NY, 1962.
5. Angel, R. J., Chopelas, A. and Ross, N. L., Stability of high density clinoenstatite at upper mantle pressure. *Nature*, 1992, **358**, 322–324.
6. Kushiro, Y., Clinopyroxenes solid solutions. Part 1. The $CaAl_2SiO_6$ component. *Jpn. J. Geol. Geogr.*, 1962, **33**, 2–4.
7. Schairer, J. F. and Yoder Jr., H. S., *Crystal and Liquid Trends in Simplified Alkali Basalts*, *Vol. 63*. Year Book, 1964, pp. 64–74.
8. Salama, S. N., Darwish, H. and Abo-Mosallam, H. A., Crystallization and properties of glasses based on diopside–Ca-Tschermak's-fluorapatite system. *J. Eur. Ceram. Soc.*, 2005, **25**, 1133–1142.
9. Höland, W. and Beall, G., *Glass–Ceramic Technology*. The Am. Ceram. Soc., Westerville, Ohio, 2002.
10. Pavlushkin, N. M., *Principals of Glass Ceramics Technology* (*2nd ed.*). Stroiizdat, Moscow, 1979 (in Russian).
11. Strnad, Z., *Glass–Ceramic Materials*. Elsevier, Amsterdam, 1986.
12. Zhunina, L. A., Kuzmenkov, M. I. and Yaglov, V. N., *Pyroxene Glass–Ceramics*. University of Minsk, 1974 (in Russian).
13. Barbieri, L., Bonamartini, A. C. and Lancellotti, A. C., Alkaline and alkaline earth silicate glasses and glass–ceramics from municipal and industrial wastes. *J. Eur. Ceram. Soc.*, 2000, **20**, 2477–2483.
14. Karamanov, A., Pelino, M. and Hreglich, A., Sintered glass–ceramics from municipal solid waste incinerator fly ashes. Part I: The influence of the heating rate on the sinter crystallization. *J. Eur. Ceram. Soc.*, 2003, **23**, 817–832.
15. Torres, F. J. and Alarcon, J., Mechanism of crystallization of pyroxene-based glass-ceramic glazes. *J. Non-Cryst. Solids*, 2004, **34**, 45–51.
16. Fergus, J., Sealants for solid oxide fuel cells. *J. Power Sources*, 2005, **147**, 46–57.
17. Loiseau, P., Caurant, D., Baffier, N., Mazerolles, L. and Fillet, C., Glass–ceramic nuclear waste forms obtained from SiO_2–Al_2O_3–CaO–ZrO_2–TiO_2 glasses containing lanthanides (Ce, Nd, Eu, Gd, Yb) and actinides (Th): study of internal crystallization. *J. Nucl. Mater.*, 2004, **335**, 14–32.
18. Loiseau, P., Caurant, D., Baffier, N., Mazerolles, L. and Fillet, C., Crystallization study of (TiO_2, ZrO_2)-rich SiO_2-Al_2O_3-CaO glasses. Part I: Preparation and characterization of zirconolite-based glass–ceramics. *J. Mater. Sci.*, 2003, **38**, 843–852.
19. Lo, C. L., Duh, J. G. and Chiou, B. S., Low temperature sintering and crystallization behaviour of low loss anorthite-based glass–ceramics. *J. Mater. Sci.*, 2003, **38**, 693–698.
20. Leonelli, C., Manfredini, T., Paganelli, M., Pozzi, P. and Pellacani, G. C., Crystallization of some anorthite-diopside glass precursors. *J. Mater. Sci.*, 1991, **26**, 5041–5046.
21. Ray, C. S., Yang, Q., Huang, W. and Day, D. E., Surface and internal crystallization in glasses as determined by differential thermal analysis. *J. Am. Ceram. Soc.*, 1996, **79**, 3155–3160.
22. Tulyaganov, D. U., Agathopoulos, S., Ventura, J. M., Karakassides, M. A., Fabrichnaya, O. and Ferreira, J. M. F., Synthesis of glass–ceramics of CaO-MgO-SiO_2 system containing B_2O_3, P_2O_5, Na_2O and CaF_2. *J. Eur. Ceram. Soc.*, 2006, **26**, 1463–1471.
23. Marques, V. M. F., Tulyaganov, D. U., Agathopoulos, S. and Ferreira, J. M. F., Low temperature synthesis of anorthite based glass–ceramics via sintering and crystallization of glass-powder compacts. *J. Eur. Ceram. Soc.*, 2006, **26**, 2503–2510.
24. Lo, C. L. and Duh, J. G., Low-temperature sintering and microwave dielectric properties of anorthite-based glass ceramic. *J. Am. Ceram. Soc.*, 2002, **85**, 2230–2235.
25. Bansal, N. P. and Gamble, E. A., Crystallization kinetics of a solid oxide fuel cell seal glass by differential thermal analysis. *J. Power Sources*, 2005, **147**, 107–115.
26. Oliveira, M., Agathopoulos, S. and Ferreira, J. M. F., Reactions at the interface between Al_2O_3–SiO_2 ceramics with additives of alkaline earth oxides and liquid Al–Si Alloy. *J. Mater. Res.*, 2002, **17**, 641–647.